Radar Precipitation Maps as Lightning Indicators

J. S. MARSHALL AND S. RADHAKANT

McGill Radar Weather Observatory, Macdonald College, Montreal, Quebec, Canada H0A 1C0

(Manuscript received 8 August 1977, in final form 22 October 1977)

ABSTRACT

Radar maps of precipitation at a height of 6 km have been studied for the thunderstorms of one July day. Regions on these maps within which the intensity level exceeds 30 dBZ (corresponding to a rainfall rate of 2.8 mm h^{-1}) represent thunderstorms, some single-celled and some multi-celled. These were found to be the sources of lightning observed (as "sferics") by a radio direction finder, frequency 100±50 kHz, located at the radar. The sferics rates of the storms were related closely to other storm parameters by

$$L=2.7A^{1.64}r^{-1.62},$$

where L is the number of sferics observed per minute, r the distance of the storm (km), and A the area (km^2) of the storm region as specified above. This study supports the findings of Larsen and Stansbury for an earlier day (*J. Atmos. Terr. Phys.*, 1974, 36, 1547–1553) and adds the algebraic relation.

1. Introduction

Operational and research use of "sferics," the location of thunderstorms and specifically of lightning flashes by direction-finding radio, has been going on for half a century. Not much effort was made to compare the patterns of radio-observed lightning and radar-observed precipitation, until SPARSA sferics sensors came on the market in the 1960's. The best report of the use of this equipment (in conjunction with good weather radar) is that of Hiser (1973), who provides statistical comparisons for each of three summers of observation.

Larsen and Stansbury (1974, hereafter abbreviated LS), working here at the McGill Radar Weather Observatory, compared radio-observed lightning flashes (sferics) with radar-observed precipitation. For the lightning, a 10 kHz radio direction finder was located at the observatory, alongside the radar. For the precipitation, the recorded data were displayed in vertical and horizontal sections, with contour lines for precipitation intensity levels 23, 43 and 63 dBZ, corresponding to rainfall rates of 1, 18 and 316 mm h^{-1}. The vertical sections revealed "precipitation cores" at a height of several kilometers as the most likely sources of the observed lightning. They also suggested that 43 dBZ contours on 7 km Constant Altitude Plan Position Indicator (CAPPI) maps would outline these cores. [The technique of these CAPPI maps has been described more recently by Marshall and Ballantyne (1975)]. Good correlation was found in time and azimuth between the recorded sferics and the cores as displayed on the 7 km CAPPI maps, which we shall refer to as "Larsen regions." (Further comparison was made on strip charts with azimuth and time as rectangular axes.) With a sequence of maps every 10 m over a 6 h period, 25 such regions have been found to be log-normally distributed in duration about a median of 30 min, with standard deviation corresponding to a factor 2.5. With these durations, the shortest-lived third must have been single cell thunderstorms, the longest-lived third multiple-cell thunderstorms. In any case, the good correlation with lightning indicates that the regions, based on radar observation of precipitation, gave a good representation in time and map location of that day's thunderstorms, with regard both to precipitation and to lightning. The total area within the 43 dBZ contour was always small in comparison with the surrounding area of lighter precipitation within the 23 dBZ contour. More details are given in a thesis (Larsen, 1973).

The LS findings appear to have relevance in both pure and applied meteorology. If developed to become more quantitative and less empirical, they should lead to improved understanding of the physical relation between precipitation and lightning. Developed technologically for real-time application, and tested over a variety of weather situations, they can make thunderstorm tracking by weather radar relevant to electrical activity as well as precipitation.

The present work extends the LS findings, particularly by obtaining a quantitative relation between the sferics rate, normalized for range, and the storm area more or less as specified by LS, i.e., the area of the Larsen region. They felt that with a single radio site problems and errors would result because only the direction of the lightning was known (and even that

0021-8952/78/0206-0212$05.00

without sense as between opposite directions). They had searched among a season's records and found only a few situations that appeared adequately free of ambiguities. As we see it, their finding has in itself changed the situation. We have sacrificed those cases where the radar indicates more than one Larsen region in the same direction (or its opposite). We have found few sferics in directions with no Larsen region within radar range (about 300 km), and our studies of range effects suggest that these should indeed be relatively few. Most of the LS data came from one July day in 1971, while ours have come from one July day in 1976. For 1976 the radar data are on digital tape, amenable to numerical mapping by computer, but the lightning records still require laborious transcription from film. For 1978 it is hoped to have both radar and radio data on the same digital tape. At that time, extension of the sort of work reported here, from a few days to many, can be realized. For the present, we must make the most of intensive study of small samples.

2. Numerical CAPPI maps

In the first study of the thunderstorms of 27 July 76, Lo (1977) used numerical CAPPI's, one every 5 min, in which each digit in a close-spaced array indicated the maximum intensity for an oblong area 4.8 km×7.5 km, so that a square printout 8 inches to the side mapped an area of 480 km×480 km centered on the radar. Fig. 1 is an outline map based on such a numerical CAPPI at 6 km, where the temperature was −17°C. (LS had chosen an altitude of 7 km somewhat arbitrarily, as a height at which to detect precipitation cores; Lo adopted 6 km because it happened to be one of a set of standard heights.) The free-form outlines (of four bands of precipitation) are for intensity level 16 dBZ, corresponding to rate of rainfall 0.4 mm h^{-1}. For the higher intensity "storm regions," rectangular outlines (following the oblongs of the numerical map) have been drawn around regions with intensity level >38 dBZ, corresponding to a rainfall rate of 9 mm h^{-1}. This sort of precipitation pattern persisted from 0900 to 1800 EST, and during that period a cold front (its surface position shown in the figure) was moving across the region.

Lightning was monitored by two radio direction finders located at the radar. One of these, the record of which was analyzed for the whole period, had been developed by Blais (1977) at IREQ (Institut de recherche de l'Hydro Québec). Its crossed-loop antennas and a field-sensing whip were tuned to 10 kHz. In the 550 min period of study, 1267 flashes were recorded. Almost all of these could be attributed to Larsen regions on the radar map, when the range of that map was extended out to 360 km. The other radio direction finder was 20 times more sensitive. The analysis of its record, for just one hour, is discussed at length in the next section.

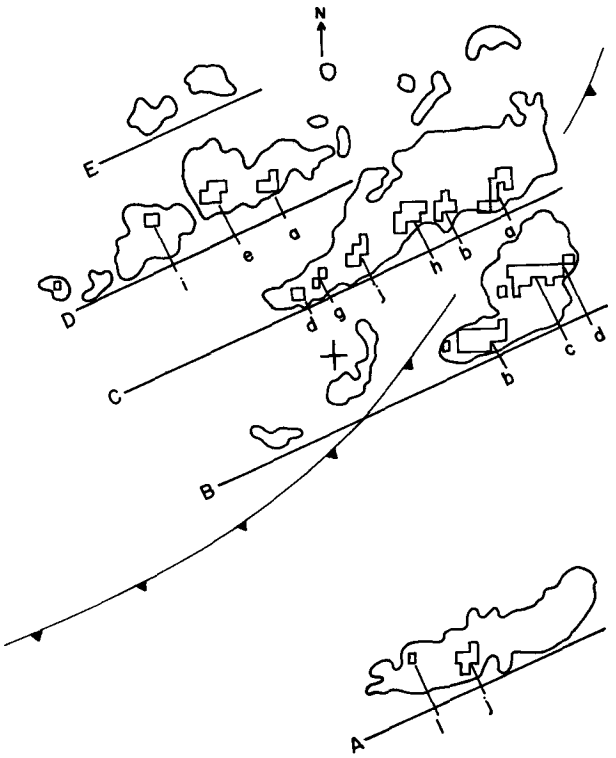

FIG. 1. CAPPI map at 6 km, 1405 EST 27 July 76. Distance from radar (marked by +) to arrowhead (N) is 240 km. Free-style outlines are for threshold intensity level 16 dBZ, corresponding to a rainfall rate of 0.4 mm h^{-1}. Smaller areas in rectangular outline are "storm regions", or "Larsen regions," containing intensity levels >38 dBZ, corresponding to a rainfall rate of 9 mm h^{-1}. The surface location of the passing cold front is also shown.

Forty-four "storm regions" such as those of Fig. 1, and which did prove to be thunderstorms, occurred during the 9 h period, with lifetimes totaling 100 h. These storms had a median lifetime of 100 min. For lifetimes up to twice the median, the observations fit a log-normal distribution, with standard deviation corresponding to a factor 4.4 (Fig. 2). Use of a lower threshold than LS (38 dBZ instead of 43 dBZ) could explain our longer lifetimes. With the lower threshold, some storms will have been multi-celled storms which, with a higher threshold, might have been observed as sequences of separate single cells.

Lifetimes longer than 200 min fell short of those on the log-normal distribution: some storms went beyond the boundary of the map, and there was a general dying-out of storms at about 1800 EST. Fig. 3 shows ten of the longer storm tracks. The direction of motion is generally from the west, with a small component from the south in the morning swinging around during the afternoon to a stronger component from the north. No consistency is apparent in the variation of storm size along the track.

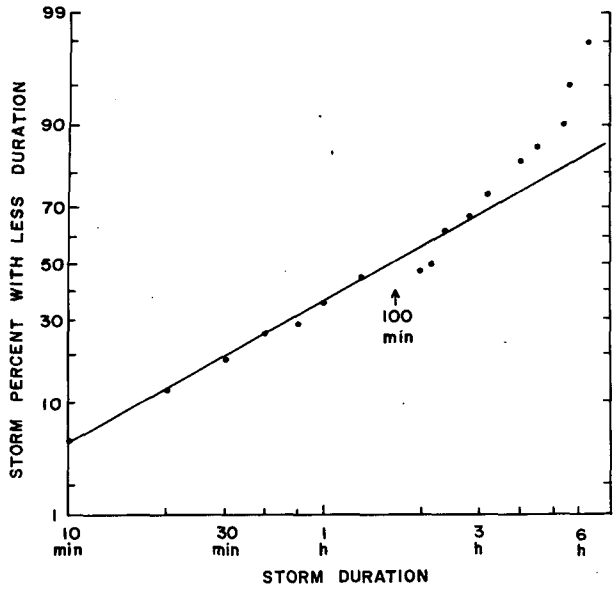

FIG. 2. Fraction percent of storm regions with lifetimes less than values indicated on axis. The straight-line locus is that of a log-normal distribution about median 100 min, with standard deviation corresponding to a factor of 4.4 in lifetime.

3. Lightning observed by radio at 100 kHz

The radio direction-finding system used by LS has been developed further (principally toward better multiple-station operation) and is still in use, with one of the stations at the radar. Data for 1976 were not available in real time, and were obtained after the event by reading a cathode ray tube display as photographed on 16 mm film. For the hour 1350 to 1450 EST on 27 July 76, the film for the station at the radar has been analyzed to yield 4500 flashes, almost 20 times as many at 100 kHz as the IREQ device recorded at 10 kHz.

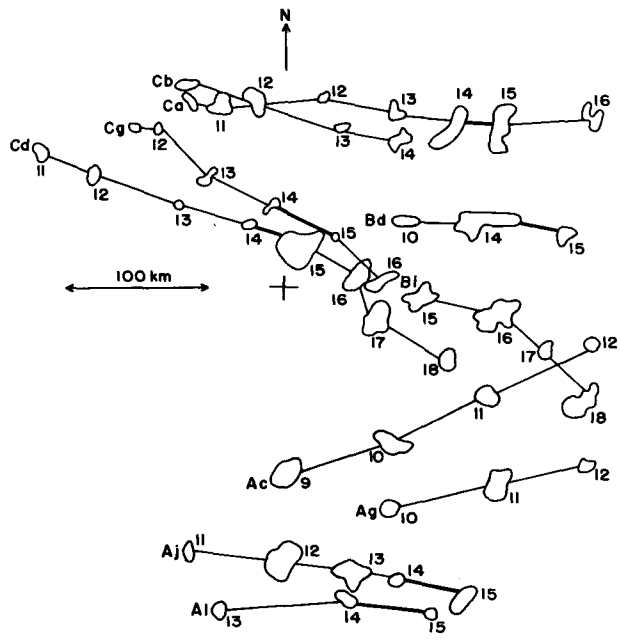

FIG. 3. Ten of the longer storm tracks. The storm region is shown for each hour, and the hour indicated. Tracks have been drawn more heavily for 1400–1500, the period of 100 kHz sferics analysis.

For comparison, the horizontal precipitation pattern at 6 km (−17°C) has been displayed on an AZLOR map in order to have all available resolution. This conformal map (Marshall and Ballantyne, 1975) has azimuth and log-range as rectangular coordinates: hence the name AZLOR. In Fig. 4, a small section of the AZLOR map at 5 min intervals gives 1) the precipitation pattern in plan for a layer at heights 6±1 km, and 2) the corresponding distributions with azimuth of lightning flashes. Marked changes from one frame to the next are apparent in both lightning and precipitation. There is not an obvious correlation of details between the lightning and precipitation patterns, and we are led to suspect that precipitation at greater or lesser heights is also contributing to the lightning.

In describing the work of LS, we have given the name "Larsen region" to the region on a CAPPI at a specified height bounded by a contour of specified intensity level. For LS, the height was 7 km, the level 43 dBZ. For the work reported in this section we specify a height of 6 km, a level of 30 dBZ, and continue to use the name. The distributions with azimuth of all the lightning and of the areas of all the Larsen regions are shown in Fig. 5. The data from these distributions have been gathered into thunderstorms, so that the sferics rate (L) and the area (A) of the Larsen region (precipitation area at height 6 km) could be compared storm by storm at 12 times during the hour. The thunderstorms are indicated by letters, with broken lines indicating the limits for the precipitation histogram (outline only, above) and the lightning histogram (cross-hatched, below). One-third of the data has been omitted from the comparison, generally because there was precipitation at two quite different ranges in the same direction.

Fig. 6 is a regression plot of $\log L$ against $\log A$, where the digit marking each point is the approximate distance of the storm from radar and radio, in units of 20 km. Two loci have been drawn, one for range 2, i.e., 40±10 km, and one for ranges 6 and 7, i.e., 130±20 km. These have slopes 1.69 and 1.77 with coefficients of determination of 0.82 and 0.83. Loci for other ranges were less good, because the data extended over shorter scales. From the separation of the two loci that have been drawn, the sferics rate varies with $r^{-1.66}$, where r is the range.

Fig. 7 is a regression plot of a trial function $\log A^{1.67}L^{-1}$ vs $\log r$. It is likely that the best locus here would increase in slope with r, but the best straight line has slope 1.62 and a coefficient of determination of 0.73. Using this slope to normalize range to 100 km, we have

$$L_1/L = (r/100\text{ km})^{1.62}, \quad (1)$$

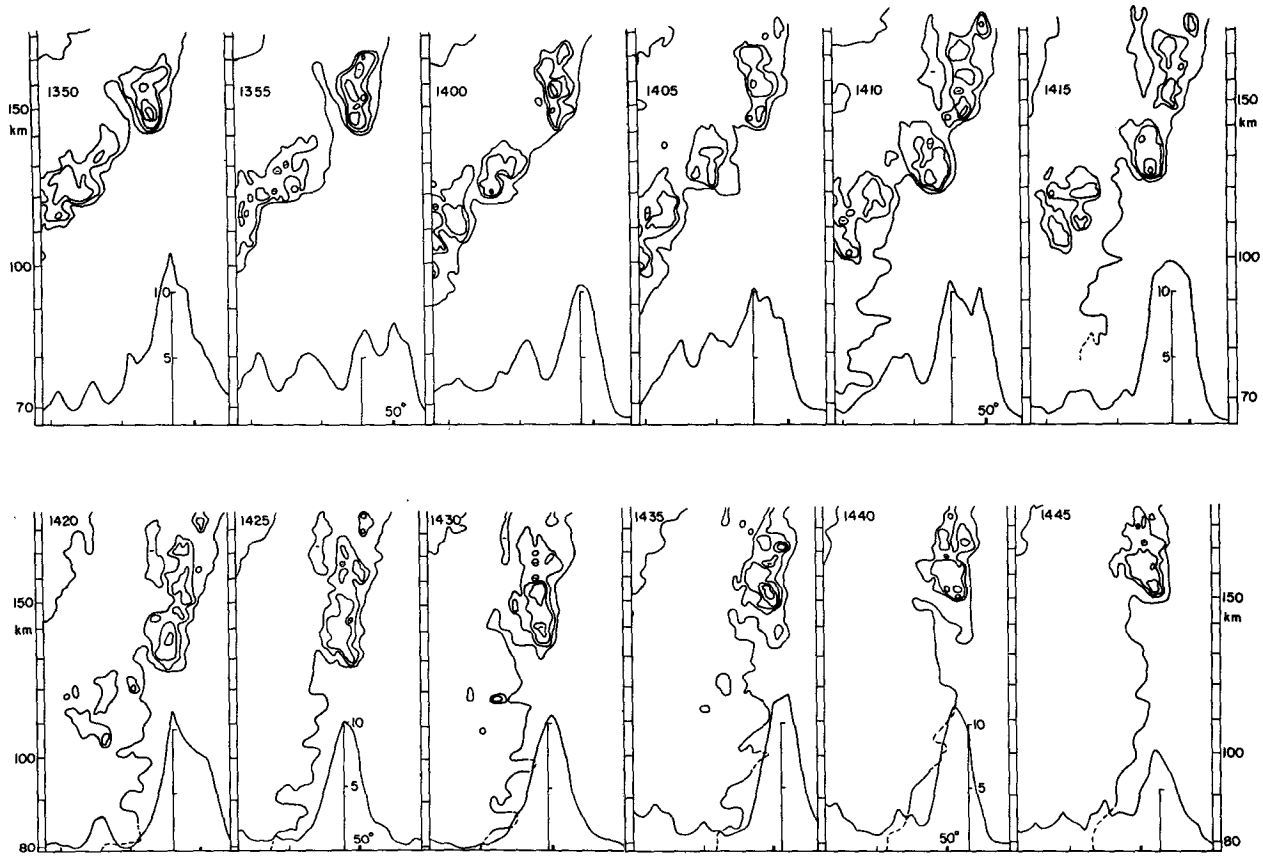

FIG. 4. Each of 12 frames contains (i) an AZLOR map, with azimuth (roughly 30–50°) as abscissa and log-range as ordinate, and (ii) distribution with azimuth of the number of sferics per degree during the 5 min interval, the number scale marked at 5 and 10. Map is conformal and storms are small enough to be mapped in true plan. The first contour line is for 16 dBZ (0.4 mm h^{-1}), the rest for 30, 38, 46 and 54 dBZ, corresponding to rainfall rates of 3, 9, 27 and 87 mm h^{-1}. The "Larsen region" bounded by 30 dBZ contains two or three rapidly varying cells outlined by 38 or 46 dBZ.

where L_1 is the sferics that would be observed at range 100 km. Accepting this relation, a regression plot of log L_1 against log A (Fig. 8) yields the locus

$$L_1 = 0.0078A^{1.64}, \quad (2)$$

where L_1 is the number of sferics that would be observed in 5 min by the 100 kHz radio direction finder at range 100 km, and A is the horizontal area at a height of 6 km (temperature −17°C) within which the intensity level of the precipitation exceeds 30 dBZ, corresponding to a rainfall rate of 2.8 mm h^{-1}. The coefficient of determination of this locus is 0.91. For the points of Fig. 8, the ratio $L_1/A^{1.64}$ has a log-normal distribution, the standard deviation corresponding to a factor of 1.62. Thus it can be seen that the radar-observed precipitation pattern, which gives the locations of the thunderstorms that are the sources of the observed lightning, also gives, for each storm, the flash rate of the lightning, or specifically the range-normalized sferics rate.

More briefly, combining (1) and (2) gives the general relation

$$L = 2.7A^{1.64}r^{-1.62}, \quad (3)$$

where L is the number of sferics per minute, r the distance (km) of the storm and A the area of the Larsen region, as specified in (2).

4. Sferics from beyond radar range

We had expected sferics from storms within radar range to be fewer than those from greater distances, but found instead that most sferics that were observed could be attributed with confidence to storms within the usual radar range (240 km) and practically all within the augmented radar range (360 km). It is worth applying to the situation the range effect reported above, based on observations at ranges 20 to 200 km, but extrapolated to several hundred kilometers. The results are as follows:

FIRST: sferics from a single storm. If we specify 100 sferics min^{-1} at a range of 100 km, then at ranges of 200, 300 and 400 km we can expect 33, 17 and 11 flashes min^{-1}.

SECOND: a random array of thunderstorms extending out indefinitely, numerous enough that random variations in the number of storms within the range of the

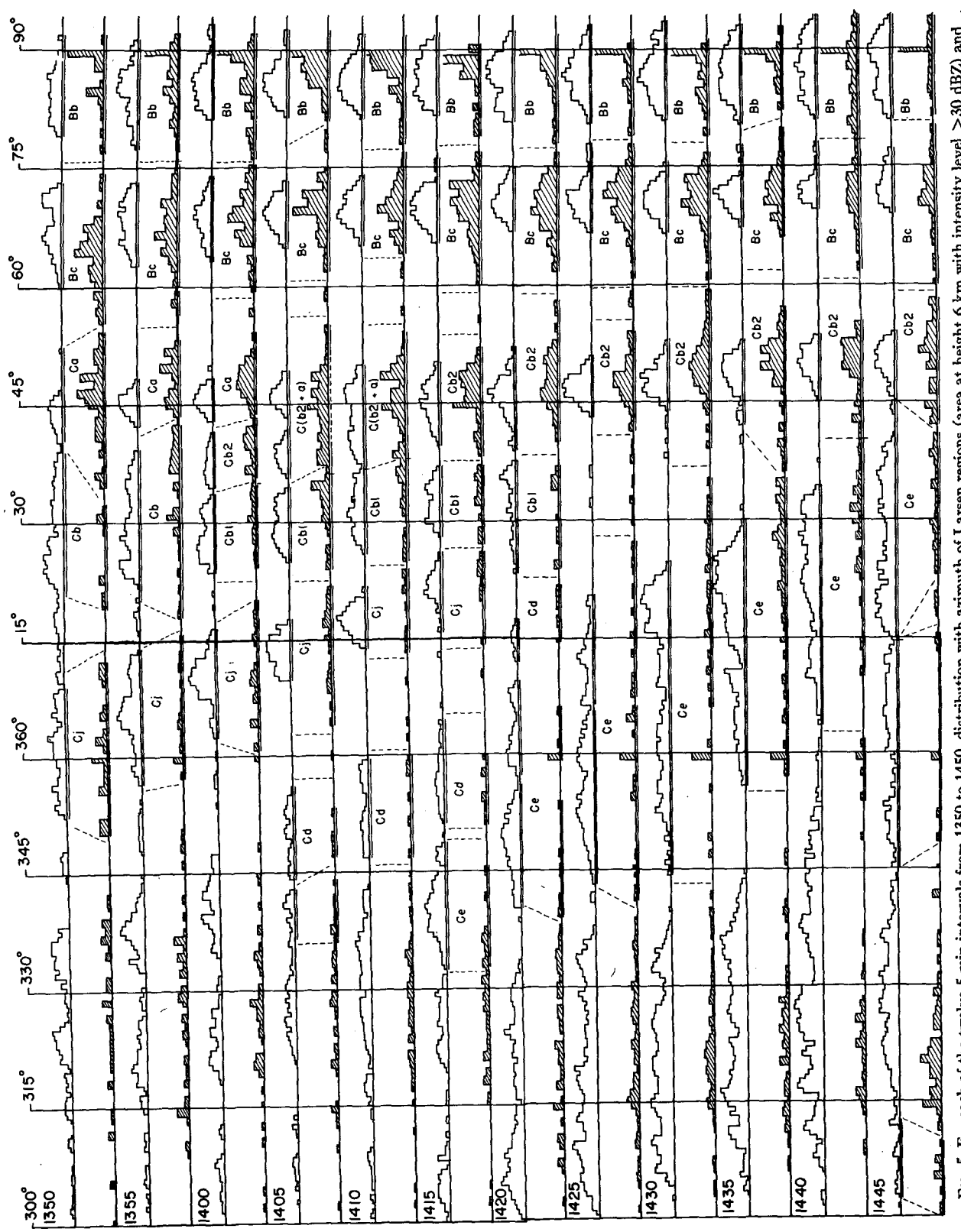

FIG. 5. For each of the twelve 5 min intervals from 1350 to 1450, distribution with azimuth of Larsen regions (area at height 6 km with intensity level >30 dBZ) and lightning (sferics recorded by 100 kHz radio in 5 min). For each 5 min, the upper histogram, in outline, gives the Larsen regions, while the lower histogram, cross-hatched, gives the lightning. Regions considered as separate storms are bounded by broken lines and lettered. One-third of the diagram was not treated in this way because two or three storms at the same bearing had different ranges.

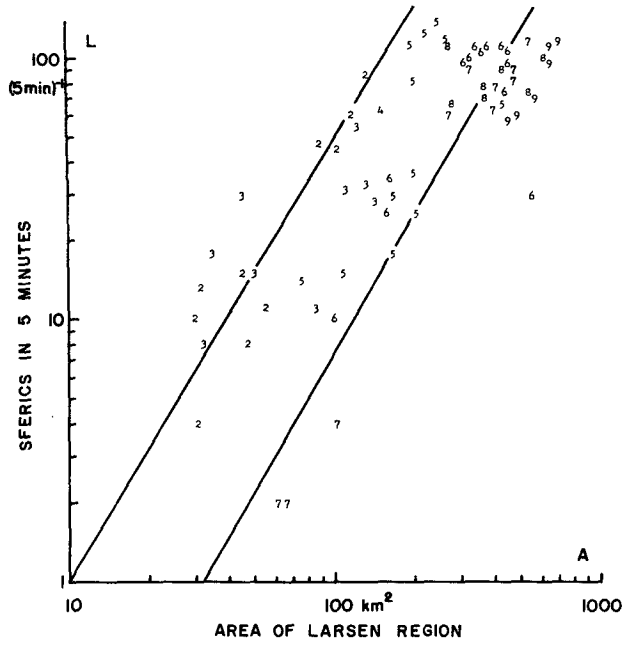

FIG. 6. Regression plot of L against A on logarithmic scales. For each point, L and A have been accumulated for one Larsen region and one 5 min interval. The digits that are used to locate the points give the range in units of 20 km. The locus drawn for range 2 has a slope of 1.69, that for ranges 6 and 7 a slope of 1.77. From the separation of the two loci, we obtain $L \propto r^{-1.66}$, where r is the range.

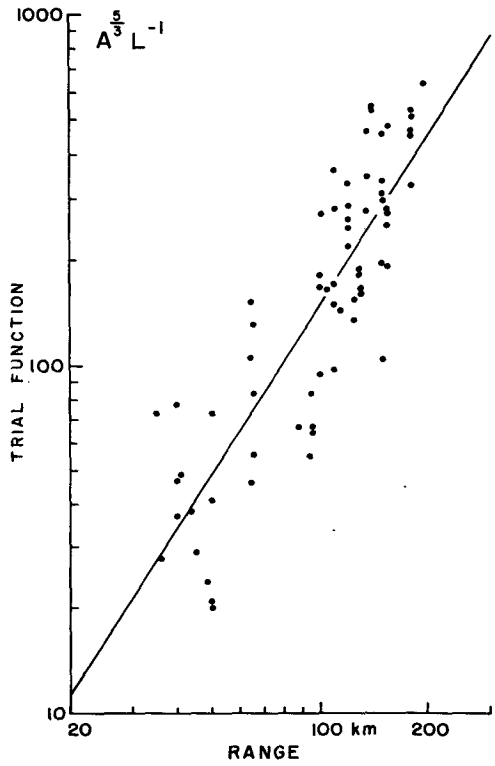

FIG. 7. Regression plot of trial function against range on logarithmic scales, to determine range effect. The data would seem to justify a curved locus, but the best straight line has slope 1.62.

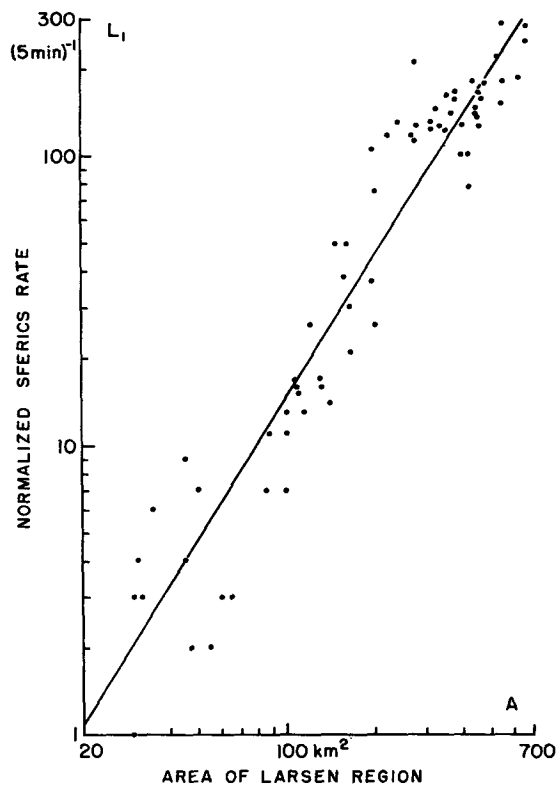

FIG. 8. Regression plot of L_1 (normalized sferics rate) against A (area of Larsen region) yielding locus $L \propto A^{1.64}$. The scatter is small enough that L_1 can be predicted from A within a factor of 2.

radar map are not great. Then for every 100 flashes from storms at ranges 20 to 240 km, there should be 50 from ranges 240 to 480 km; and for every 100 flashes from storms at ranges 20 to 360 km, there should be just 45 from ranges 360 to 720 km. Such extensive random arrays in two dimensions are unlikely at any one time, but are reasonable for a seasonal accumulation.

THIRD: thunderstorms distributed along a line extending out indefinitely. For simplicity, the line is taken to pass through the observatory. For 100 sferics coming from ranges 20 to 240 km, there should be 10 from ranges 240 to 480 km; and for 100 sferics coming from ranges 20 to 360 km, there should be 7 coming from ranges 360 to 720 km.

In summary, the range effect that we have found at a frequency of 100 kHz suggests that when there is considerable lightning associated with storms within radar range, the sferics from these storms are likely to exceed those from greater ranges. The ratio of the number of sferics from beyond radar range to the number within radar range is more likely to be of the order of 10% than it is to be of the order of 50%.

5. Summary and conclusions

Larsen and Stansbury (1974) generated radar maps of precipitation at a height of 7 km (−30°C) at 10 min intervals. On these they outlined regions within which

the precipitation intensity level exceeded 43 dBZ. A comparison of these regions, replotted against coordinates of azimuth and time, with lightning flashes (recorded by a 100 kHz radio direction finder), showed that the regions were sources of these flashes throughout 90% of their lives, and that they could account for 75% of the flashes observed. The regions were thus the map representations of thunderstorms or, more often, of individual convective cells within thunderstorms.

We have repeated the work of LS, with maps at a height of 6 km (−17°C) at 5 min intervals, with outlines at intervals of 4 dBZ from 30 to 58 dBZ, for 27 July 1976. Regions within 38 dBZ outlines had longer lifetimes (median 100 min, standard deviation of log-normal distribution corresponding to a factor 4.4) than those of LS; apparently they were generally the map representations of the convectively-active regions of thunderstorms, whether the region consisted of a single cell or was a compact assembly of a small number of interactive cells. Lightning flashes recorded by a relatively insensitive 10 kHz direction finder could almost all be attributed to the radar-observed regions within 38 dBZ outlines.

For comparison with flashes recorded at 100 kHz (by an improved version of the LS equipment), the storm region within the 30 dBZ outline was considered. A relation was found among the area A of this "Larsen region," its distance r from the observatory and its sferics rate L, measured over 5 min intervals. The sferics rate L, at fixed range or normalized for range, was found to vary as $A^{1.64}$ [Eq. (2) and (3)], and the range-normalized value of L could be predicted within a factor of 2 from the value of A (Fig. 8).

We recognize that the quantity A is only an empirical parameter of electrical activity. Further, its use to a power of about 5/3 can be embarrassing, on occasions when the breaking down of a precipitation map into storm regions of area A involves arbitrary decisions. Possibly $A^{1.64}$ could be replaced by the product Ah, where h would be height above some elevated base height; that would give the storm region three dimensions instead of two.

For applied meteorology, apparently a weather-radar map of precipitation can be generated which can be read directly as a map of electrical activity, and for this purpose the empirical parameter A may be appropriate. Toward this end, detailed study on single days should give way to testing on many days and in different climates; for this, digital tape recording of the radio data as well as of the radar data is a desideratum. Pakiam and Maybank (1975) note a difference in the electrical behavior of super-cell and multiple-cell thunderstorms, and this difference would have to be taken into account, for example.

Acknowledgments. Mr. Lo Cheuk-Wai made the first comparison of the radar data reported here, with 10 kHz sferics. He also transcribed film records to provide the 100 kHz data used here. We are grateful to him and to Mrs. Eva Cherna, who made a large contribution to the subsequent analysis. We gratefully acknowledge financial support by the National Research Council of Canada, and by the Québec Department of Education under their programme *Formation de chercheurs et d'action concertée.*

REFERENCES

Blais, René, 1977: Système de détection angulaire de la foudre. *Trans. Can. Elect. Assoc. Eng. Oper. Div.*, **16**, Part IV, Paper no. 77-TC-200.

Hiser, H. W., 1973: Sferics and radar studies of south Florida thunderstorms. *J. Appl. Meteor.*, **12**, 479–483.

Larsen, H. R., 1973: Studies of thunderstorms by sferics and radar. Sci. Rep. MW-79, McGill Weather Radar Observatory, Macdonald College Post Office, Quebec. This is a McGill University Ph.D. thesis.

Larsen, H. R., and E. J. Stansbury, 1974: Association of lightning flashes with precipitation cores extending to height 7 km. *J. Atmos. Terr. Phys.*, **36**, 1547–1553.

Lo, Cheuk-Wai, 1977: Lightning and precipitation interrelated for a stormy day. M.Sc. thesis, McGill University, 45 pp.

Marshall, J. Stewart, and Ernest H. Ballantyne, 1975: Weather surveillance radar. *J. Appl. Meteor.*, **14**, 1317–1338.

Pakiam, J. E., and J. Maybank, 1975: The electrical characteristics of some severe hailstorms in Alberta, Canada. *J. Meteor. Soc. Japan*, **53**, 363–383.